Numerical Simulation of Phase Transformations in Shape Memory Alloy Thin Films

Debiprosad Roy Mahapatra and Roderick V.N. Melnik

Mathematical Modelling and Computational Sciences,
Wilfrid Laurier University, Waterloo, ON, N2L3C5, Canada

Abstract. A unified variational framework and finite element simulations of phase transformation dynamics in shape memory alloy thin films are reported in this paper. The computational model is based on an approach which combines the lattice based kinetics involving the order variables and non-equilibrium thermodynamics. Algorithmic and computational issues are discussed. Numerical results on phase nucleation under mechanical loading are reported.

1 Introduction

Phase transforming solids, in particular metallic alloys with large differences in lattice constants of their crystollographic variants have interesting properties. The variants (phases) which exist at low temperature are called martensites and the parent state which exists at high temperature is called austenite. When temperature is increased, the martensites are transformed to austenite at certain critical temperature. Further, when mechanical force is applied at constant temperature, the structure undergoes a different transformation path from austenite to martensites and recovers the original shape. This is known as shape memory effect. The associated strain can be quite large $(6\% - 50\%)$ depending upon the size of the sample. Shape memory effect has wide range of applications in mechanical, bio-medical and micro-device engineering. Due to thermomechanically coupled phase transformation which is not diffusive but of first-order type, and which produces microstructures with sharp interfaces with large rotations of lattice vectors, the experimental, analytical and computational characterization of the material properties and overall structural responses become highly challenging. There are three important mathematical and computational issues for reliable numerical simulation of shape-memory alloys, which are (1) an accurate description of the free energy density, its frame-invariance and material symmetry properties [1, 2], (2) prediction of the microstructures [2, 3] and their evolutions [4, 5, 6] and (3) prediction of the thermo-mechanical hysteresis at the macroscopic scale, which is important in the numerical simulation based design of shape-memory alloy devices [7]. Therefore, a challenging task is to address all of the above objectives systematically within a *unified* modeling, analysis and computational framework. In this paper we report a finite element based numerical simulation of phase transformations in shape memory alloy thin films. The computational model is based on a Ginzburg-Landau free energy description,

detailed analytical studies of which can be found in [8, 9, 10, 11]. Applications of the Landau theory to the description of first-order martensitic phase transitions can be found in [12]. Also, numerical simulations of microstructure due to cubic to tetragonal transformation in thin films based on continuum theory of lattice have been reported [3], where quadratic polynomial of the strain invariants have been employed to construct the free energy densities separately for the austenite and the martensites. In the above work, a free-boundary type variational formulation was employed for quasi-static analysis of microstructure.

In order to perform numerical simulations, we have developed a variational framework and a finite element code, wherein a general thermo-mechanical loading can be handled while studying the lattice-based kinetics of the microstructures. The computational model developed here employs a variational framework, where the thermodynamic conservation law couples the mechanical deformation, temperature and the order variables. The order variables describe the type of phase (parent austenite phase or a martensitic variant) at a material point. The paper is structured as follows. In Sec. 2, we summarize the Ginzburg-Landau free energy coupled model, which has been implemented in the variational framework. The variational framework and the finite element formulation are discussed in Sec. 3. Computational issues are discussed in Secs. 4 and 5. Numerical results for cubic to tetragonal phase transformations in Ni-Al thin films are reported in Sec 6.

2   Ginzburg-Landau Free Energy Model

We denote the order variables $\eta_k \in [0, 1]$, where $k = 1, \cdots, N$ indicates the number of martensitic variants, $\eta_k = 0 \, \forall k$ defines the austenite and $\eta_k = 1$, $\eta_j = 0$, $k \neq j$ defines the kth martensitic variant at a material point. According to the point group of crystallographic symmetry, only one type of martensite is allowed to exist at a material point. Denoting the vector of the order variables as $\boldsymbol{\eta} = \{\eta_1, \cdots, \eta_N\}^T$, the Gibbs free energy density is defined as $G(\boldsymbol{\sigma}, \theta, \boldsymbol{\eta})$. Here $\boldsymbol{\sigma}$ is the stress tensor, θ is the temperature. The finite strain tensor $\boldsymbol{\varepsilon}$ is decomposed into the elastic part and the transformation-induced part as

$$\boldsymbol{\varepsilon} = \boldsymbol{\varepsilon}_{\text{el}} + \sum_{k=1}^{N} \boldsymbol{\varepsilon}_k^t \varphi(\eta_k) \, , \tag{1}$$

where $\varphi(\eta_k)$ is a polynomial in η_k and $\boldsymbol{\varepsilon}_k^t$, $k = 1, \cdots, N$ are the transformation strain tensors [2] obtained using experiments. The structure of the initially unknown polynomial $\varphi(\eta_k)$ is such that it satisfies the following two conditions:

$$\varphi(0) = 0 \, , \quad \varphi(1) = 1 \, . \tag{2}$$

The frame-invariance property of the free energy density is imposed by the polynomial structure in η_k such that interchanges between two indices produce identical structure of G. Material symmetry under proper rotation of the lattice

vector is preserved due to the decomposition in Eq. (1). The Gibbs free energy density then takes the following form.

$$G(\eta) = -\frac{1}{2}\boldsymbol{\sigma} : \left[\boldsymbol{\lambda}_0 + \sum_{k=1}^{N}(\boldsymbol{\lambda}_k - \boldsymbol{\lambda}_0)\varphi(\eta_k)\right] : \boldsymbol{\sigma} - \boldsymbol{\sigma} : \sum_{k=1}^{N}\boldsymbol{\varepsilon}_k^t\varphi(\eta_k)$$

$$- \boldsymbol{\sigma} : \left[\boldsymbol{\varepsilon}_{\theta 0} + \sum_{k=1}^{N}(\boldsymbol{\varepsilon}_k^\theta - \boldsymbol{\varepsilon}_0^\theta)\varphi(\eta_k)\right] + \sum_{k=1}^{N}f(\theta,\eta_k) + \sum_{i=1}^{N-1}\sum_{j=i+1}^{N}F_{ij}(\eta_i,\eta_j) , \quad (3)$$

where $\boldsymbol{\lambda}_k$ is the second-order forth-rank compliance tensor for the kth martensitic variant (M_k phase), $\boldsymbol{\lambda}_0$ is for austenite phase (A phase), $\boldsymbol{\varepsilon}_0^\theta = \boldsymbol{\alpha}_0(\theta - \theta_e)$, $\boldsymbol{\varepsilon}_k^\theta = \boldsymbol{\alpha}_k(\theta - \theta_e)$. θ_e is the temperature at which the stress-free martensite losses stability. $\boldsymbol{\alpha}_0$ and $\boldsymbol{\alpha}_k$ are the thermal expansion tensors for A and M_k phases, respectively. $f(\theta,\eta_k)$ is the chemical part of the free energy of the M_k phases and assumed in the form of a polynomial which is to be determined. F_{ij} is an interaction potential required to preserve the frame-invariance of G with respect to the point group of symmetry and uniqueness of the multivariant phase transformation at a given material point. The description of the order variables can now be generalized with three sets of order parameters: $\bar{0} = \{0, \eta_k = 0, 0\}$ for A phase, $\bar{1} = \{0, \eta_k = 1, 0\}$ for M_k phase and $\bar{\eta}_k = \{0, \eta_k, 0\}, \eta_k \in (0,1)$ for diffused $A - M_k$ interface. The role of the first-order kinetics in the order variables is to assist in reaching the bottom of the energy well, i.e.,

$$\frac{\partial G}{\partial \eta_k} = 0 , \quad \boldsymbol{\eta} = \bar{0}, \bar{1} , \tag{4}$$

$$\frac{\partial^2 G}{\partial \eta_k^2} \le 0 , \quad \boldsymbol{\eta} = \bar{0} \quad (A \to M_k), \tag{5}$$

$$\frac{\partial^2 G}{\partial \eta_k^2} \le 0 , \quad \boldsymbol{\eta} = \bar{1} \quad (M_k \to A). \tag{6}$$

The transformation energy associated with $A \leftrightarrow M_k$ transformation is

$$G(\boldsymbol{\sigma}, \theta, \bar{0}) - G(\boldsymbol{\sigma}, \theta, \bar{1}) = \boldsymbol{\sigma} : \boldsymbol{\varepsilon}_k^t - \Delta G^\theta , \tag{7}$$

where ΔG^θ is the jump in the free energy due to phase transformation. With the help of Eqs. (2)-(7), we determine $\varphi(\eta_k)$ and $f(\theta,\eta_k)$ (see [10] for the details). According to Landau theory, a quadratic polynomial in strain components can be adequate to describe the free energy. Therefore, following Eq. (1), one finds that for cubic to tetragonal transformation, the interaction potential has the following form (see [9] for the details)

$$F_{ij} = \eta_i\eta_j(1 - \eta_i - \eta_j)\left[B\left\{(\eta_i - \eta_j)^2 - \eta_i - \eta_j\right\} + D\eta_i\eta_j\right] + \eta_i^2\eta_j^2(\eta_i Z_{ij} + \eta_j Z_{ji})$$
$$\tag{8}$$

where the material constants B and D are obtained from experiments or numerical estimation. The matrix elements Z_{ij} are obtained as functions of the constants B and D and an energy scale factor in $f(\theta,\eta_k)$.

2.1   Thermodynamic Conservation

Note that a jump in the free energy ΔG^θ has been introduced in Eq. (7). The consequence of this jump, as well as the jump in the total strain across the $A-M_j$ interface, is the thermodynamic forcing as a source of dissipation. The forcing term would eventually be balanced by the kinetic force. Therefore, one has to establish a link between the evolution of the phases and the non-negativity of the thermodynamic potential (Helmholtz free energy). This is unlike the notion in plasticity-based framework (see e.g.[13]), where the non-negativity of the rate of phase fraction is directly enforced.

For the present problem, the kinetic equation is derived by balancing the thermodynamic force with the kinetic force as

$$C\frac{\partial \eta_k}{\partial t} + \frac{\partial G'}{\partial \eta_k} = 0 \; , \tag{9}$$

where C is a constant and $G' = G + \tilde{G}(\nabla\boldsymbol{\eta})$ describes the modified Gibbs free energy including the gradient terms to account for the non-local nature of the interface energy. By rearranging Eq. (9) and expanding the forcing terms, we get the Ginzburg-Landau equation for phase kinetics, which is given by

$$\frac{\partial \eta_k}{\partial t} = -\sum_{p=1}^{N} L_{kp}\left[\frac{\partial G}{\partial \eta_p} + \boldsymbol{\beta}_p : \boldsymbol{\nabla}\boldsymbol{\nabla}\eta_p\right] + \theta_k \; , \tag{10}$$

where L_{kp} are positive definite kinetic coefficients, $\boldsymbol{\beta}_p$ are positive definite second rank tensor. θ_k is the thermal fluctuation satisfying the dissipation-fluctuation theorem. Eq. (10) is complemented by the macroscopic energy conservation law

$$\frac{\partial}{\partial t}\left[\mathcal{W} - \theta\frac{\partial \mathcal{W}}{\partial \theta}\right] - \boldsymbol{\nabla}\cdot(\boldsymbol{\sigma}\cdot\dot{\boldsymbol{u}} - \boldsymbol{q}) = h_\theta \; , \tag{11}$$

and the momentum balance equation

$$\rho\frac{\partial^2 \boldsymbol{u}}{\partial t^2} = \boldsymbol{\nabla}\cdot\boldsymbol{\sigma} + \boldsymbol{p} \; , \tag{12}$$

where $\mathcal{W}$ is the Helmholtz free energy given by

$$\mathcal{W} = G + c_v\theta + \frac{1}{2}\boldsymbol{\sigma} : \left[\boldsymbol{\lambda}_0 + \sum_{k=1}^{N}(\boldsymbol{\lambda}_k - \boldsymbol{\lambda}_0)\varphi(\eta_k)\right] : \boldsymbol{\sigma}$$

$$+ \boldsymbol{\sigma} : \left[\boldsymbol{\varepsilon}_{\theta 0} + \sum_{k=1}^{N}(\boldsymbol{\varepsilon}_{\theta k} - \boldsymbol{\varepsilon}_{\theta 0})\varphi(\eta_k)\right] \; , \tag{13}$$

$\boldsymbol{q}$ is the heat flux, h_θ is the heat source and $\boldsymbol{p}$ is body force.

3   Variational Framework and Finite Element Discretization

We relate the elastic part of displacements to the elastic strain $\boldsymbol{\varepsilon}_{\text{el}}$ via the linear strain-displacement relation, i.e. $\boldsymbol{\varepsilon}_{\text{el}} = ((\nabla\boldsymbol{u}) + (\nabla\boldsymbol{u})^T)/2$. With this assumption of strain and Eq. (1), it is now obvious that the order variables $\eta_k, k = 1, \cdots, N$, are to be treated as internal variables in the variational formulation. We want to interpolate the fields $\boldsymbol{u}(x, y, z, t)$, $\theta(x, y, z, t)$ and $\eta_k(x, y, z, t)$ over the domain $\Omega(x, y, z) \subset R^2$ with Lipschitz continuous boundary $\partial\Omega$, using fixed-order finite elements with h-refinement. We consider the Lagrangian isoparametric interpolation function $\boldsymbol{N}$,

$$\{u_1, \ u_2, \ u_3\}^T = \boldsymbol{N}_u \boldsymbol{v}^e , \quad \theta = \boldsymbol{N}_\theta \boldsymbol{v}^e , \quad \eta = \boldsymbol{N}_\eta \boldsymbol{v}^e , \tag{14}$$

$$\boldsymbol{v} = \{u_1, \ u_2, \ u_3, \ \theta, \ \eta_1, \cdots, \eta_n\}^T . \tag{15}$$

Here, the superscript e indicates element nodal quantities. Introducing admissible weights $\{\bar{u}_i, \bar{\theta}, \bar{\eta}_k\}$ chosen from the linear span of $\boldsymbol{v}^e$, the variational formulation of the problem can be stated as follows

$$\delta\Pi = \delta\Pi_{\text{PT}} + \delta\Pi_\theta + \delta\Pi_u + \delta W = 0 , \quad t \in [0, +\infty] \tag{16}$$

where

$$\delta\Pi_{\text{PT}} = \int_\Omega \sum_{k=1}^N \sum_{p=1}^N \delta\bar{\eta}_k \left[L_{kp} \left(\frac{\partial G}{\partial \eta_p} + \boldsymbol{\beta}_p : \nabla\nabla\eta_p \right) \right] \mathrm{d}\mathbf{x}$$

$$\int_\Omega \sum_{k=1}^N \delta\bar{\eta}_k \left[\frac{\partial \eta_k}{\partial t} - \theta_k \right] \mathrm{d}\mathbf{x} - \int_{\partial\Omega} \sum_{k=1}^N \sum_{p=1}^N \delta\bar{\eta}_k L_{kp} \frac{\partial G}{\partial \eta_k} \mathrm{d}s(\mathbf{x}) , \tag{17}$$

$$\delta\Pi_\theta = \int_\Omega \delta\bar{\theta} \left[\frac{\partial}{\partial t} \left(\mathcal{W} - \theta \frac{\partial \mathcal{W}}{\partial \theta} \right) - \nabla \cdot \left(\boldsymbol{\sigma} \cdot \frac{\partial \boldsymbol{u}}{\partial t} \right) \right] \mathrm{d}\mathbf{x}$$

$$+ \int_\Omega \delta\bar{\theta} \left[\nabla \cdot \left(-\kappa\nabla\theta - \alpha'\kappa\nabla \frac{\partial \theta}{\partial t} \right) \right] \mathrm{d}\mathbf{x} - \int_{\partial\Omega} \delta\bar{\theta} \boldsymbol{q}_\perp \mathrm{d}s(\mathbf{x}) , \tag{18}$$

$$\delta\Pi_u = \int_\Omega \delta\bar{\boldsymbol{u}}^T \left[\rho \frac{\partial^2 \boldsymbol{u}}{\partial t^2} - \nabla \cdot \boldsymbol{\sigma} \right] \mathrm{d}\mathbf{x} - \int_{\partial\Omega} \delta\bar{\boldsymbol{u}}^T \boldsymbol{\sigma}_\perp \mathrm{d}s(\mathbf{x}) , \tag{19}$$

and W is the external work done over the sample. Integrating Eq. (16) by parts, we obtain the finite element approximation

$$\boldsymbol{M} \frac{\partial^2 \boldsymbol{v}}{\partial t^2} + \boldsymbol{D} \frac{\partial \boldsymbol{v}}{\partial t} + \boldsymbol{K}\boldsymbol{v} = \boldsymbol{f} , \tag{20}$$

with initial state and microstructure

$$\boldsymbol{v}(\boldsymbol{t}) = \boldsymbol{v}(0) , \quad \frac{\partial}{\partial t} \boldsymbol{v}(t) = \boldsymbol{0} . \tag{21}$$

4   Deformation, Phase Kinetics and Multiple Scales

The problem of simulating the microstructure in shape memory alloys has been extensively discussed in the literature [1], primarily under static loadings. Dynamic loadings present a major remaining challenge in the field. While simulating the macroscopic deformation under dynamic loadings, resolving the sharp interfaces and the dendritic microstructure with multiscale features are some of the key computational difficulties that need to be addressed. A smoothed version of the transformation conditions in Eqs. (4)-(6) leads to the time-dependent Ginzburg-Landau phase kinetics, where the fast time scale has to be controlled depending on the global time stepping (in slow time scale) in the finite element time integration. Note that η_k represents the reordering of the atomic ensemble within a box (or in other words within a finite element). Choice of the length-scale for defining this box can be arrived at by applying a finite-difference scheme to the phase kinetic equation. The chosen time scale for the kinetics dictates the limit to the coarse graining of η_k. This, in turn, restricts the order of interpolation for a given size of the finite element. Since the elastic part of the strain is defined in the lattice coordinate for the current phase, special care is necessary to ensure continuity of elastic strain and hence displacement within that phase. For example, if linear interpolation is used for displacement and there exists a number of elements having same phase connected to a finite element node, then we average out the displacement for that particular node. For higher-order interpolation, this is not necessary, except when additional intermediate nodes are used in an element for interpolation of η_k.

5   Computational Scheme

We have implemented the finite element model discussed in Sec. 3 in a general three-dimensional finite element code. For numerical simulation of cubic to tetragonal transformation, we deal with three different phases, that is $N = 3$. We employ an 8-node, 7 d.o.f/node hexahedral element with tri-linear isoparametric interpolation and reduced Gauss-quadrature integration for in-plane shear terms. Since the energy minimization process can take a different and unphysical path, a special care should be taken in organizing nonlinear iterations. The implemented algorithm is given below.

(1) Form the matrix $\boldsymbol{M}$ and the linear parts of the matrices $\boldsymbol{D}$ and $\boldsymbol{K}$.

(2) Time step: $t_i = t_0$; Form the nonlinear system. Solve: $\boldsymbol{K}(\boldsymbol{v}_i)\boldsymbol{v}_{i+1} = \bar{\boldsymbol{f}}(\boldsymbol{v}_i)$.

(3) Iteration step : $j = 1$; From (2), $\boldsymbol{v}_{i+1}^j = \boldsymbol{v}_{i+1}$. Form $\Delta\bar{\boldsymbol{f}}_{i+1}^j = \bar{\boldsymbol{f}}(\boldsymbol{v}_{i+1}^j)_{\text{int}} - \bar{\boldsymbol{f}}(\boldsymbol{v}_i)$. Solve [14]: $\Delta\boldsymbol{v}_{i+1}^{j+1} = -\boldsymbol{K}(\boldsymbol{v}_{i+1}^j)^{-1}\Delta\bar{f}_{i+1}^{j}$.

(4) Update: $\boldsymbol{v}_{i+1}^{j+1} = \boldsymbol{v}_{i+1}^j + \Delta\boldsymbol{v}_{i+1}^{j+1}$. Check stability conditions Eqs. (5)-(6). If not consistent, update η_k only and repeat (3).

(5) Update: $\boldsymbol{\varepsilon}_{i+1}^{j+1}$, $\boldsymbol{\sigma}_{i+1}^{j+1}$. Check convergence. If not converged $j \leftarrow j + 1$, repeat (3) else go to (6).

(6) Update: $\dot{\boldsymbol{v}}_{i+1} = \dot{\boldsymbol{v}}_{i+1}^{j+1}$, $\ddot{\boldsymbol{v}}_{i+1} = \ddot{\boldsymbol{v}}_{i+1}^{j+1}$. $i \leftarrow i + 1$, repeat (2).

6   Numerical Simulations

A Ni-Al thin film is considered for numerical analysis in this section as an example. The material properties are taken from [9]. $5Hz$ sinusoidal stress is applied in the longitudinal direction throughout the left and right edges of the rectangular film. The stress distribution over the edge has equilateral triangular shape. The other two parallel edges of the film are kept free. Constant temperature of $300K$ with cubic phase (austenite) is assumed to be the initial state. Figures 1 and 2, respectively, show the displacements and the nucleated phases near the stressed left and right edges of the film.
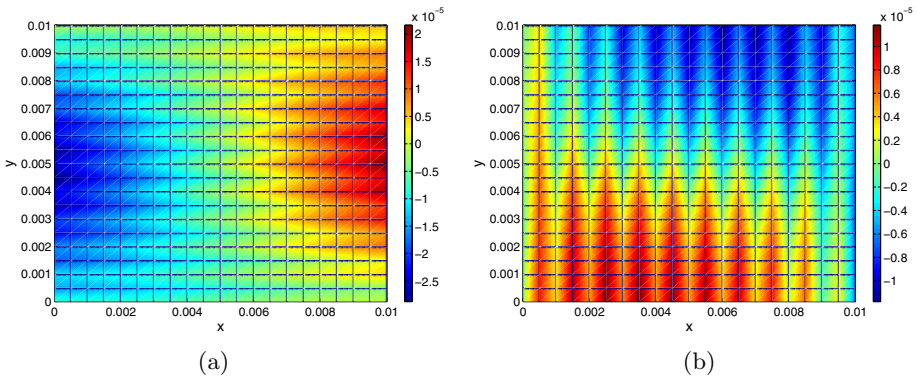

(a)   (b)

Fig. 1. (a) Longitudinal displacement u_1 and (b) lateral displacement u_2 during nucleation of the martensites from the right edge at the first one-fourth of the loading cycle $(t = 25ms)$
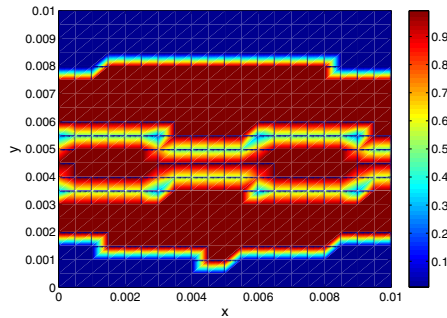

Fig. 2. Martensitic variant $\eta_1 \rightarrow 1$ (seen as the horizontal strips in the middle) during nucleation from the left and right edges at the first one-fourth of the tensile loading cycle $(t = 25ms)$

7   Conclusions

A computational model has been developed and the simulations based on this model capture a qualitative behaviour of the Ni-Al microstructure observed experimentally (see [15]).

References

1. J.M. Ball and C. Carstensen, Compatibility conditions for microstructures and the austenite-martensite transition, *Mater. Sci. and Eng. A*, 273, 231-236 (1999).
2. K. Bhattacharya, *Microstructure of Martensite*, Oxford University Press (2003).
3. P. Belik and M. Luskin, Computational modeling of softening in a structural phase transformation, *Multiscale Model. Simul.*, 3(4), 764-781, (2005).
4. R. Abeyaratne, C. Chu and R.D. James, Kinetics of materials with wiggly energies: The evolution of twinning microstructure in a Cu-Al-Ni shape memory alloys, *Phil. Mag.*, 73A, 457-496 (1996).
5. A. Artemev, Y. Wang, A.G. Khachaturyan, Three-dimensional phase field model and simulation of martensitic transformation in multilayer systems under applied stresses, *Acta Mater.*, 48, 2503-2518 (2000).
6. T. Ichitsubo, K. Tanaka, M. Koiwa and Y. Yamazaki, Kinetics of cubic to tetragonal transformation under external field by the time-dependent Ginzburg-Landau approach, *Phy. Rev. B*, 62, 5435 (2000).
7. F. Auricchio and L. Petrini, A three-dimensional model describing stress-temperature induced solid phase transformations: solution algorithm and boundary value problems, *Int. J. Numer. Meth. Engng.*, 61, 807-836, (2004).
8. V.I. Levitas and D.L. Preston, Three-dimensional Landau theory for multivariant stress-induced martensitic phase transformations. I. Austenite $\leftrightarrow$ martensite, *Phys. Rev. B*, 66, 134206 (2002).
9. V.I. Levitas, D.L. Preston and D.W. Lee, Three-dimensional Landau theory for multivariant stress-induced martensitic phase transformations. III. Alternative potentials, critical nuclei, kink solutions, and dislocation theory, *Phys. Rev. B*, 68, 134201 (2003).
10. D.R. Mahapatra and R.V.N. Melnik, A dynamic model for phase transformations in 3D samples of shape memory alloys, *LNCS* Springer-Verlag, 3516, 25-32 (2005).
11. D. Roy Mahapatra and R.V.N. Melnik, Finite element approach to modelling evolution of 3D shape memory materials, *Math. Computers Simul.* (submitted) Sep 2005.
12. F. Falk and P. Kanopka, Three-dimensional Landau theory describing the martensitic phase transformation of shape-memory alloys, *J. Phys.: Condens. Matter*, 2, 61-77 (1990).
13. J.G. Boyd and D.C. Lagoudas, A thermodynamical constitutive constitutive model for shape memory materials. Part I. the monolithic shape memory alloy, *Int. J. Plasticity*, 12(6), 805-842, 1996.
14. J.C. Simo and T.J.R. Hughes, Computational Inelasticity, Springer-Verlag, 1997.
15. P. Boullay, D. Schryvers and J.M. Ball, Nanostructures at martensite macrotwin interfaces in $Ni_{65}Al_{35}$, *Acta Mater.*, 51, 1421-1436, 2003.